Radar–Radiometer-Based Liquid Water Content Retrievals of Warm Low-Level Clouds: How the Measurement Setup Affects Retrieval Uncertainties

Nils Küchler and Ulrich Löhnert

***Abstract*—Here, we propose a new methodology that increases the understanding of uncertainty sources of liquid water content (LWC) retrievals, which are caused by the combination of instruments having different beam widths and are horizontally displaced. Furthermore, we give first quantitative uncertainty estimates. This paper is based on a case study of a single-layer, warm, stratiform cloud observed at the Jülich Observatory for Cloud Evolution. The LWC profiles of this cloud have been forward-simulated with the passive and active radiative transfer model providing radar and microwave radiometer (MWR) observables for all cloud columns. These observables have been converted back into LWC profiles, whereas, in this case, the MWR and radar observables from different columns were combined, representing horizontal displacement. We investigate the influence of horizontal distance between a radar and an MWR on a commonly used retrieval for LWC, which scales radar reflectivity profiles with the liquid water path given by the MWR. We found that a displacement of only 10 m already introduces an additional relative uncertainty of 10%. At 100 m displacement, the relative error grows up to 30%. Additionally, different beam widths decrease the retrieval accuracy by a few percent; however, at large displacements, radiometers with larger beam widths slightly decrease the error due to the displacement. Finally, we show that cloud edge studies require optimally matched beams between the radar and the radiometer, and already a displacement of 10 m leads to unreasonable results.**

***Index Terms*—Ground-based remote sensing, liquid water content (LWC) retrievals, microwave radiometer (MWR), radar, sensor synergy, uncertainty.**

I. Introduction

LOW level clouds, such as stratus and stratocumulus, cover a large area of the planet and thereby strongly influence the Earth's radiation budget [1]. In general, clouds are a major uncertainty source in numerical weather and climate prediction models [2], and therefore, clouds must be correctly characterized by observations to enable accurate model validation. Furthermore, advancing model resolutions in space and time [3] increases the demand for highly resolved retrievals of cloud properties, such as liquid water content (LWC) with well-quantified uncertainty estimates.

Long-term observations of LWC with temporal and spatial resolutions of a few seconds and meters, respectively, can be recorded using ground-based remote sensing. A common approach to retrieve LWC is to combine radar with microwave radiometer (MWR) measurements by scaling the vertical reflectivity profile (Z_e) derived from a radar with the column liquid water path (LWP) derived from an MWR [4], [5]. Both instruments are standard equipment at measurement sites observing cloud processes and properties [6]–[9] and are used mostly by the community to retrieve LWC profiles [10].

Retrievals are always associated with uncertainties that: can be instrument specific, such as calibration bias, instrument noise, and finite bandwidths [11], [12]; can be caused by inherent retrieval assumptions and algorithm uncertainties [5], [13]; and can be caused by combining two instruments, which may lead to mismatching sampling volumes [14]. The latter is often assumed to be of minor importance, especially, when temporal averaging to several seconds or minutes is applied. However, when conducting high-frequency sampling (e.g., 1 Hz), different half power beamwidths (HPBW) and horizontal distance between two senors (henceforth "sensor displacement ΔX") can affect the retrieval accuracy.

Current state-of-the-art cloud radars have HPBWs varying between 0.2° and 0.58° [15]–[17], whereas state-of-the-art MWRs, retrieving LWP, span a range from 0.58° to 6° HPBW [17]–[19]. Information on ΔX is often not discussed or not given at all in literature describing comprehensive observatories and campaigns [8], [20], although it can range from about 10 m [21] up to about 100 m [22], and which has significant influence on the retrieval accuracy.

When combining a radar and a radiometer, being displaced by 100 m and both vertically pointing, and having a HPBW of 0.5°, the observed volumes of the two instruments will intersect at 5.7 km the first time. Thus, if low-level clouds are present, also the sampling volumes will be horizontally displaced, i.e., the two sensors will observe different scenes, e.g., at 1.5-km height the volumes are displaced by 75 m. That radar and radiometer observe different scenes can also happen in case of overlapping beams, namely, if the sensors have very different HPBWs.

Manuscript received March 30, 2018; revised October 8, 2018 and January 30, 2019; accepted March 16, 2019. Date of publication May 21, 2019; date of current version May 25, 2019. This work was supported by the project Energy Transitions and Climate Change (http://et-cc.uni-koeln.de/project.html) of the Excellence Initiative of the University of Cologne by the German Research Foundation (DFG) under Grant ZUK 81/1. Observations used in this study originate from DFG funded Core Facility (Jülich Observatory for Cloud Evolution—Core Facility) under DFG Research Grant LO 901/7-1. *(Corresponding author: Nils Küchler.)*

The authors are with the Institute for Geophysics and Meteorology, University of Cologne, 50923 Cologne, Germany (e-mail: nkuech@meteo.uni-koeln.de; loehnert@meteo.uni-koeln.de).

Color versions of one or more of the figures in this paper are available online at http://ieeexplore.ieee.org.

Digital Object Identifier 10.1109/JSTARS.2019.2908414

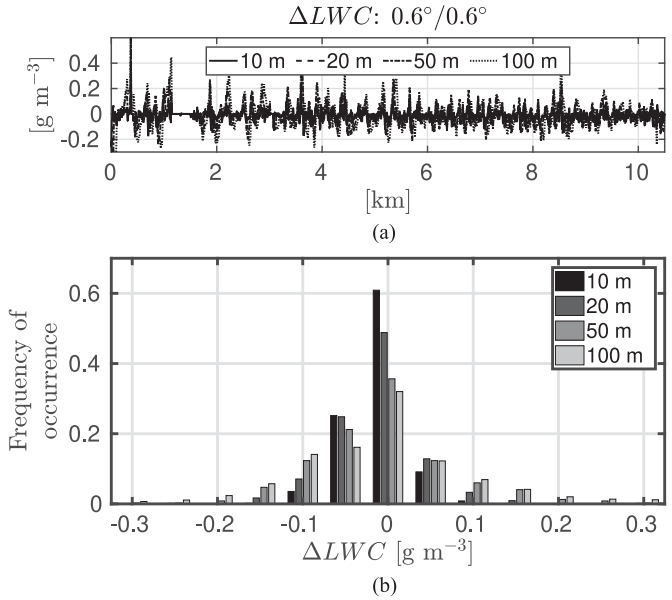

Fig. 1. Error of LWC retrieval (ΔLWC) combining radar and MWR measurements after [13] that was applied to the reference cloud in Fig. 2(a). The error is caused by displacing (here 10, 20, 50, 100 m) radar and MWR from each other, both having a HPBW of 0.6°. (a) Error at maximum of the LWC profile in the cloud. (b) Frequency of occurrence of ΔLWC shown in (a) depending on different displacements.

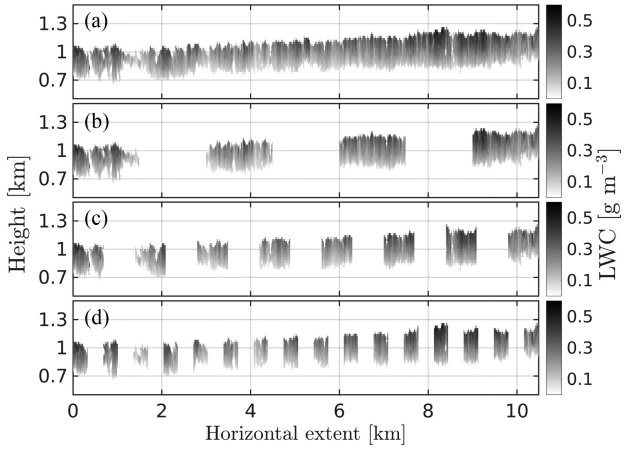

Fig. 2. (a) Reference cloud (RefCloud) that has been created applying reflectivity and LWP measurements to (1). The measurements were recorded by a W-band radar–radiometer at the JOYCE—CF in Jülich, Germany. (b) Slices of RefCloud of (a) to mimic a broken cloud field. (c) Like in (b), but two times more and smaller slices. (d) Like in (c), but two times more and smaller slices.

A radar–radiometer combination having HPBWs of 0.2° and 6°, respectively, with $\Delta X = 0$ m has overlapping beams; however, the footprint of the radiometer is 1000 times larger than the footprint of the radar at any height. Hence, any variability in the observed column will be less pronounced in the radiometer signal than in the column integrated radar signal.

Fig. 1 illustrates the effect of ΔX on a retrieval at the maximum of an LWC profile (LWC_{max}) when combining a radar and an MWR having both an HPBW of 0.6°. The time series exhibits how much LWC_{max} differs from a reference LWC_{max}, i.e., at $\Delta X = 0$ m, for different sensor displacements. Deviations above 0.4 g m^{-3} (about 300% relative error) are visible, being on average larger for a larger ΔX. Such under or overestimations can lead to strong under or overestimations of cloud top radiative cooling of several Kelvin per hour [23].

In the following, we will discuss the effects of ΔX and differences in the HPBWs on LWC retrievals of warm low-level stratiform clouds, which combine radar and radiometer measurements. Thereby, it is assumed that the LWC can be correctly derived after [13] given that both instruments observe the identical field of view. We further investigate how these differences influence the retrieval at cloud edges and when broken cloud fields are present.

II. Methodology

The following analysis is based on the LWC retrieval by [13] combining MWR and radar measurements. Thereby, the square root of Z_e is scaled with the LWP providing an LWC estimate for the ith layer after

$$\text{LWC}_i = \text{LWP}\frac{\sqrt{Z_i}}{\sum_{j=1}^{M} \Delta h_j \sqrt{Z_j}}. \quad (1)$$

Each of the M layers is associated with a reflectivity Z_i and a vertical resolution Δh_i. Equation (1) can be applied as long as the cloud droplet number concentration is constant within the cloud and the third moment of the drop size distribution (DSD) is linearly related to the sixth moment of the DSD. Both assumptions were found to be valid in warm, non-drizzling stratus clouds [13].

Assuming that (1) holds, a reference cloud (henceforth "RefCloud"), containing only cloud droplets, was created by converting a 1-h time series of Z_e and LWP into a two-dimensional spatial field of LWC [see Fig. 2(a)]. The Z_e and LWP time series have been recorded at the Jülich Observatory for Cloud Evolution—Core Facility (JOYCE—CF) [8] with a W-band radar–radiometer measuring with temporal and vertical resolutions of about 3 s and about 20 m [17], respectively. At JOYCE-CF, the so-called CLOUDNET classification product [7] is available, which classified the cloud as containing cloud droplets only.

Although the data of the W-band radar–radiometer has been recorded every 3 s, the actual sampling time was 1 s. Cloud base was located at about 800 m within this hour exhibiting a wind speed of about 10 m s^{-1}. The footprint of the radar has a diameter of about 6 m at 800 m. On the basis of these values, we assumed that the radar averaged over approximately 10 m horizontal cloud extent, hence, one data point in time corresponds to about 10 m horizontal extend in Fig. 2(a).

Considering RefCloud as the physical truth, observables such as Z_e and brightness temperatures (BTs) can be forward simulated for any radar–MWR combination exhibiting different HPBW, frequencies, and ΔX when applying some further assumptions that will be introduced later in this section. After

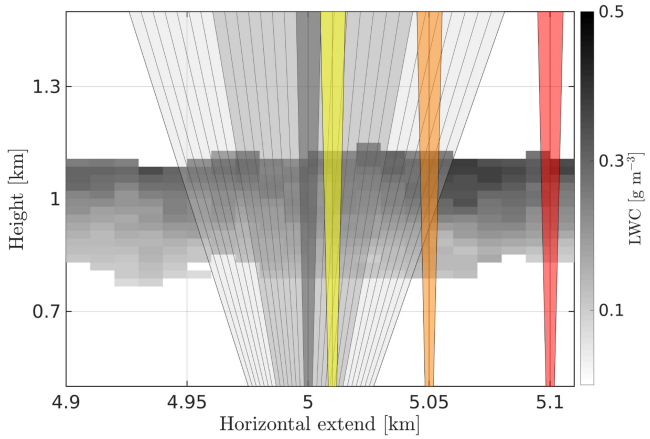

Fig. 3. Reference cloud with LWC. Fields of view from ground-based remote sensing instruments, here radar and radiometer, are shown in gray, red, orange, and yellow. Gray areas represent HPBW of 6.2°, 3.5°, and 0.6°. Yellow, orange, and red have an HPBW of 0.6°, too. Instruments with gray areas are located at the ground at 5-km horizontal extent. Yellow, orange, and red represent the field of view of a radar that is displaced by 10, 20, and 50 m, respectively. Hence, a radar being displaced by 50 m observes a different scene than a radiometer with one of the gray fields of view. The solid lines within the beams indicate paths along which radar reflectivities and BTs were forward simulated using the passive and active radiative transfer model [25]. Simulations were performed at all horizontal grid points, being spaced by 10 m. In addition to the LWC, a log-normal DSD and an effective radius increasing from 5 to 9 μm from the cloud base to cloud top were assumed. Finally, these observables can be converted back into LWC profiles using (1) while assuming different displacements between radar (reflectivity) and MWR (BTs). The derived LWC profile can be then compared to the profiles of the reference cloud.

determining LWP combining the forward simulated BTs at several frequencies [24], LWC profiles can be determined again following (1).

Fig. 3 illustrates the geometrical concept of our study: because of finite beam widths, the sensors receive signal from cloud regions not directly located in the vertical field of view of the sensor, which is typically the scene of interest. The larger the HPBW, the more regions out of interest contribute to the measured signal. Forward simulations were performed at 31 angles equally spaced (in radian) between -3.1° and $+3.1^\circ$ along slanted paths providing 31 BTs and Z_e profiles. Final (averaged) Z_e profiles and BTs were calculated for different HPBWs, i.e., averaging a different number of slanted path simulations while assuming a perfect Gaussian antenna pattern to weight contributions differently from different directions. Note that we neglected any effects due to antenna side lobes. Moreover, the radar HPBW used here corresponds to the gain-squared pattern, i.e., the pattern resulting from a two-way propagation of radiation through the antenna, which is not the case for the radiometer where the radiation passes only once the antenna. Usually, radar HPBW are given in one-way HPBW. Comparing a one-way radar HPBW with a radiometer HPBW of the same value would lead to different fields of view because the actual radar HPBW, i.e., the gain-squared pattern, has a finer resolution than the one-way HPBW.

Instrument displacement was imitated by combining Z_e profiles and BTs from different horizontal positions (X). The instruments were displaced in steps of 10 m varying from 0 to 100 m. Thereby, the radar beam was shifted toward larger values of X with respect to the MWR, i.e., $X_{\text{radar}} > X_{\text{MWR}}$, and the column above the radar was considered as truth (lwc_{true}). Hence, the LWC profile for a displaced combination ($\text{lwc}_{\text{displaced}}$) was calculated with the LWP derived at a horizontal distance of $X_{\text{MWR}} = X_{\text{radar}} - \Delta X$ compared to the radar location.

BTs and Z_e of RefCloud were forward simulated with the passive and active microwave radiative transfer model [25] for ground-based, zenith pointing instruments at several frequencies between 21 and 35 GHz. The radar frequency and the radar Doppler spectrum noise floor at 1 km radial distance were set to 35 GHz and -38 dBZ, respectively. We assumed a log-normal-DSD with a width of 0.38 having a random uncertainty of ± 0.14 [26] and an effective radius that linearly increases from 5 μm at the cloud base to 9 μm at cloud top [14]. Note that RefCloud was constructed using data from a W-band radar without considering any attenuation effects. This might have indeed led to an (over-) under-estimation of LWC at the cloud (base) top when constructing RefCloud with respect to the actual cloud structure. However, constructing RefCloud using W-band radar data does not affect the following analysis, because Z_e profiles were simulated at 35 GHz where attenuation is negligible for an average LWP of RefCloud of about 50 gm^{-2}.

Based on the averaged BTs, LWP was retrieved using seven frequencies between 21 and 31 GHz, which are commonly used to derive LWP [27]. The retrieval is a quadratic model [17] and was developed with a training data set of 15 175 radiosondes, in which the presence of a modified adiabatic cloud was assumed when the relative humidity exceeded 95% [27]. A random uncertainty of ± 1 K was added to BTs before determining the retrieval coefficients. The uncertainty in the retrieval is characterized by a root-mean-square error (RMSE) of 25 gm^{-2}.

We used frequencies between 21 and 35 GHz to represent most accurate state-of-the-art retrievals of LWP and to minimize attenuation effects in the radar measurements. To investigate also how cloud patchiness influences the retrieval accuracy of two displaced instruments, RefCloud was sliced into broken cloud fields with different degrees of patchiness [see Fig. 2(b), (c), and (d)] before the forward simulations were performed.

III. Results

Based on the methodology explained in Section II, we derived median profiles of the relative error of LWC

$$\Delta\text{lwc}_{\text{rel}} = \frac{\text{lwc}_{\text{true}} - \text{lwc}_{\text{displaced}}}{\text{lwc}_{\text{true}}} \tag{2}$$

which will be used in the following to quantify the retrieval uncertainty depending on different measurement setups.

A. Sensor Displacement and Varying HPBWs

Figs. 4(a), (c), and (e) show the median of $\Delta\text{lwc}_{\text{rel}}$

$$\text{Md}(\Delta\text{lwc}_{\text{rel}}) = \text{median}(\Delta\text{lwc}_{\text{rel}}) \tag{3}$$

for 10, 20, and 50 m displacement depending on the in-cloud position h^* ($h^* = 0$ corresponds to cloud base and $h^* = 1$ to cloud top) and four different combinations of MWR and radar HPBWs:

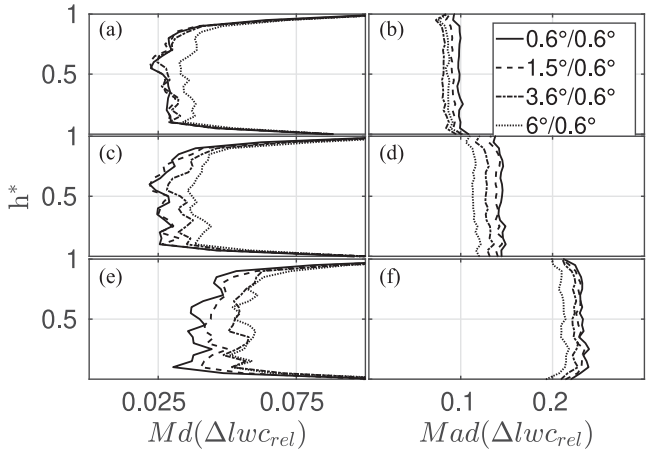

Fig. 4. Left column: Median relative error of LWC ($\mathrm{Md}(\Delta\mathrm{lwc_{rel}})$) depending on position within the cloud h^* ($h^* = 0$ (= 1) corresponds to cloud base (top)) and different combinations of radiometer/radar HPBWs. (a) 10-m displacement between radar and MWR. (c) 20-m displacement. (e) 50-m displacement. Right column: Same as left column but showing median absolute deviation of $\Delta\mathrm{lwc_{rel}}$ ($\mathrm{Mad}(\Delta\mathrm{lwc_{rel}})$). (b), (d), (f) for 10, 20, and 50 m displacement.

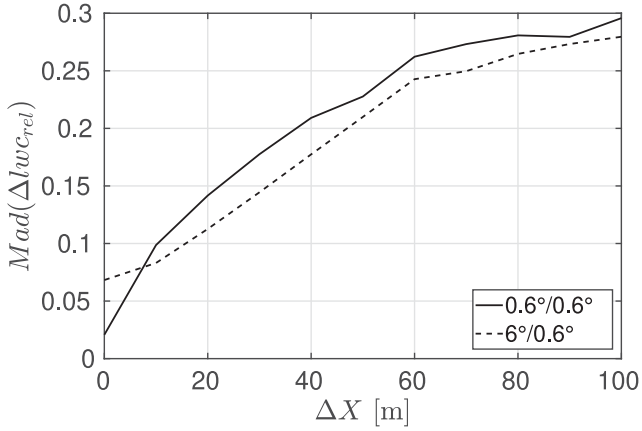

Fig. 5. Median absolute deviation of relative LWC error ($\mathrm{Mad}(\Delta\mathrm{lwc_{rel}})$) at the cloud center depending on sensor displacement ΔX and different HPBW combinations (radiometer/radar).

0.6°/0.6° (MWR HPBW/radar HPBW), 1.5°/0.6°, 3.6°/0.6°, and 6°/0.6°. We do not show different radar HPBWs, since varying the HPBW between 0.6° and 1° has no significant effect on the retrieval performance.

The profile of $\mathrm{Md}(\Delta\mathrm{lwc_{rel}})$ is approximately constant for h* values between 0.2 and 0.8. This is what is expected, since any offset in Z_e cancels out in (1) [13], thus, the remaining uncertainty from the LWP measurement (ΔLWP) leads to a constant relative error when normalizing with the LWC profile. The influence of the random uncertainty of Z_e is small compared to the effect of ΔLWP and vanishes when considering statistical averages as done in Fig. 4(a), (c), and (e). At cloud center, $\mathrm{Md}(\Delta\mathrm{lwc_{rel}})$ is larger for larger MWR HPBW and increases with ΔX. On average, $\mathrm{Md}(\Delta\mathrm{lwc_{rel}})$ increases from about 3% at $\Delta X = 10$ m to 5% at $\Delta X = 50$ m.

Close to the cloud base and cloud top, $\mathrm{Md}(\Delta\mathrm{lwc_{rel}})$ increases strongly exhibiting values of up to 12%. This is due to varying cloud base and cloud top from column to column (data point X to data point $X + \Delta X$). In the setup investigated here, a radar with an HPBW of 0.6° receives signals also from neighboring columns. Therefore, a higher (lower) cloud base (top) in the neighboring columns, i.e., volumes without signal, can lead to a strong underestimation of Z_e at cloud base (top) producing a large $\mathrm{Md}(\Delta\mathrm{lwc_{rel}})$.

The effect of different HPBWs has a magnitude similar to the sensor displacement. $\mathrm{Md}(\Delta\mathrm{lwc_{rel}})$ is about 2%–3% smaller when combining 0.6°/0.6° than the combination of 6°/0.6°. Henceforth, we refer to the HPBW combinations 0.6°/0.6° and 6°/0.6° as beam combination–narrow narrow (BC–NN) and beam combination–wide narrow (BC-WN), respectively.

When observing processes with a high temporal resolution, the median absolute deviation

$$\mathrm{Mad}(\Delta\mathrm{lwc_{rel}}) = \mathrm{median}(|\Delta\mathrm{lwc_{rel}} - \mathrm{Md}(\Delta\mathrm{lwc_{rel}})|) \quad (4)$$

which is similar to the RMSE, is a more reasonable choice as uncertainty estimate than $\mathrm{Md}(\Delta\mathrm{lwc_{rel}})$. $\mathrm{Mad}(\Delta\mathrm{lwc_{rel}})$ is about 10% at $\Delta X = 10$ m and increases to about 20% at $\Delta X = 50$ m [see Fig. 4(b), (d), and (f)]. In contrast to $\mathrm{Md}(\Delta\mathrm{lwc_{rel}})$, $\mathrm{Mad}(\Delta\mathrm{lwc_{rel}})$ is larger for BC–NN that for BC–WN, which is due to smoothing effects at larger MWR HPBWs. This will be further discussed in the following paragraph.

Fig. 5 shows $\mathrm{Mad}(\Delta\mathrm{lwc_{rel}})$ depending on ΔX for BC–NN and BC–WN at the cloud's center. Since $\mathrm{Mad}(\Delta\mathrm{lwc_{rel}})$ is approximately constant with height [see Fig. 4(b), (d), and (f)], the curve in Fig. 5 is representative for any cloud level not too close to cloud top or cloud base. For both combinations, $\mathrm{Mad}(\Delta\mathrm{lwc_{rel}})$ increases from about 5% at zero displacement to about 30% at $\Delta X = 100$ m. At $\Delta X = 0$ m, BC–NN shows a much smaller uncertainty than BC–WN, which is due to the much wider MWR beam of BC–WN averaging over several data columns and thereby smoothing the LWP signal. However, the wider beam is beneficial once radar and MWR are displaced from each other and the LWP varies on length scales of the displacement. Thus, the LWP retrieved from an MWR with a large HPBW will be on average closer to the LWP of the scene of interest than an LWP retrieved with a small HPBW. This can be seen in Fig. 5 where BC–NN has a greater $\mathrm{Mad}(\Delta\mathrm{lwc_{rel}})$ than BC–WN for any ΔX larger than zero.

A different way to assess the uncertainty of the retrieval following (1) is to investigate the correlation between the LWP and the sum of $\sqrt{Z_e}$ ($\sum\sqrt{Z_e}$) within the observed column. Both parameters are linearly related based on (1). Fig. 6(a) shows the correlation between $\sum\sqrt{Z_e}$ and LWP depending on ΔX and the HPBW combinations. It is evident that the correlation decreases with increasing ΔX, which confirms the findings that $\mathrm{Mad}(\Delta\mathrm{lwc_{rel}})$ increases with ΔX. For any HPBW combination, the correlation drops from about 0.85 to 0.58, which implies that displacing instruments decreases the validity of (1). Additionally here, we see the same effect as in Fig. 5: a larger MWR HPBW shows lower uncertainty once $\Delta X > 0$ m.

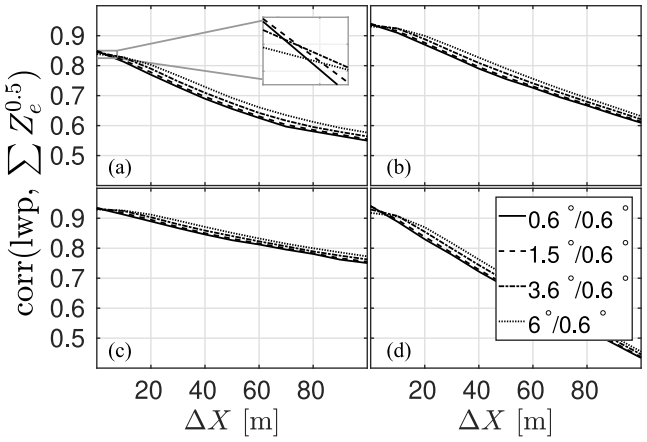

Fig. 6. Linear correlation coefficients (corr$(\cdot,\cdot)$) between the LWP and cumulative square root of reflectivity ($\sum Z_e^{0.5}$) depending on sensor displacement ΔX and different combinations of HPBW (radiometer/radar). (a)–(d) Z_e and LWP were determined from reference clouds in Fig. 2(a)–(d).

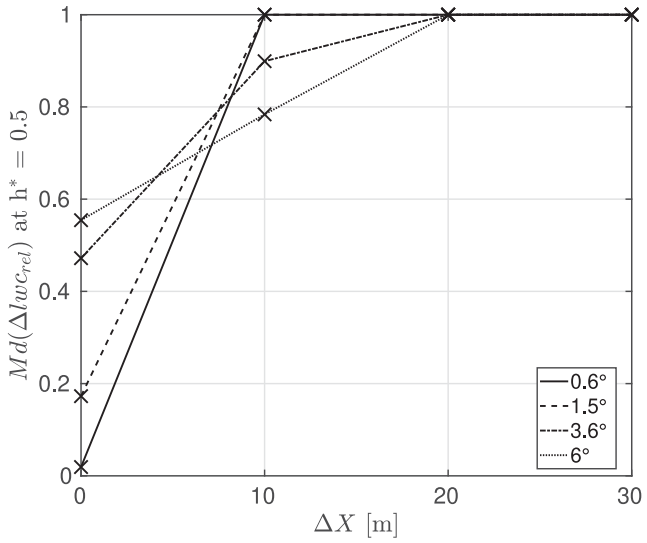

Fig. 7. Median relative error of LWC $\mathrm{Md}(\Delta\mathrm{lwc_{rel}})$ at cloud edges from Fig. 2(d) depending on sensor displacement ΔX. The error curve is determined at cloud center, i.e., at $h^* = 0.5$. $\mathrm{Md}(\Delta\mathrm{lwc_{rel}}) = 1$ indicates that no LWC profile could be derived due to sensor displacement. The radar was located under the first cloudy column at the lateral cloud edge and the radiometer was shifted toward cloud free columns.

B. Cloud Variability and Cloud Edges

To investigate the effect of cloud variability in terms of patchiness, we sliced RefCloud into three cloud fields with different degrees of variability [see Fig. 2(b)–(d)]. Additionally, for these cloud fields, we determined the correlation between $\sum\sqrt{Z_e}$ and LWP depending on ΔX [see Fig. 6(b)–(d)]. When comparing Fig. 6(b)–(d) to Fig. 6(a), one can see that the correlation at zero displacement is always larger in broken cloud fields, which is due to the clear sky periods where both $\sum\sqrt{Z_e}$ and LWP are approximately zero. However, the correlation coefficients at $\Delta X = 100$ m are larger in Figs. 2(b)/6(b) (0.62), much larger in Figs. 2(c)/6(c) (about 0.77), but smaller in Figs. 2(d)/6(d) (0.45). The effect of larger correlation at larger ΔX in Figs. 2(b)/6(b) and Figs. 2(c)/6(c) does not reflect a decrease of retrieval uncertainty, rather an optimal matching between the window size of clear sky regions and ΔX. Hence, Figs. 2(b)/6(b) and 2(c)/6(c) do not provide usable information. However, the strong decrease of the correlation in Figs. 2(d)/6(d) compared to Figs. 2(a)/6(a) tells the following: on the one hand, the retrieval by [13] is not applicable once the cloud field varies on length scales similar to ΔX but, on the other hand, as long as ΔX is small, LWC can be retrieved also for very patchy cloud fields. Additionally, here, beam width effects are small compared to sensor displacement.

As scattering of sunlight is very complex in broken cloud fields, it is important to accurately determine the microphysics at cloud edges. To gain a first estimate of how accurate cloud edges can be described in terms of LWC by (1), we determined $\Delta\mathrm{lwc_{rel}}$ at the left cloud edges (N = 16) in Fig. 2(d). Thereby, the radar position was fixed at the first cloudy column of each cloud edge and the radiometer was shifted toward lower values of X, i.e., $X_{\mathrm{radar}} \geq X_{\mathrm{MWR}}$. Since the LWC of the radar column was used to normalize the error [see (2)], we considered only left cloud edges to obtain non-infinite error estimates. Hence, the maximum possible value of $\Delta\mathrm{lwc_{rel}}$ is 1 (100%). Fig. 7 illustrates the median of $\Delta\mathrm{lwc_{rel}}$ ($\mathrm{Md}(\Delta\mathrm{lwc_{rel}})$) depending on the HPBW of the MWR and ΔX at cloud center, i.e., at $h^* = 0.5$. $\Delta\mathrm{lwc_{rel}}$ is 100% once the MWR does not provide an estimate for LWP, hence, no LWC can be retrieved although the radar observes the cloud edge. One can see that almost for any combination of HPBW and $\Delta X > 0$, the retrieval does not provide any information. Only the MWR–HPBW of 3.6° and 6° provide information on LWP at $\Delta X = 10$ m. Yet, $\mathrm{Md}(\Delta\mathrm{lwc_{rel}})$ is larger than 70% implying that in these cases the beam of the MWR is only partially filled by the cloud.

IV. Conclusion

Our analysis provides relative uncertainty estimates of LWC after [13] for varying distances between radar and MWR and HPBWs of both, as well as the impact in overcast versus broken cloudy scenes. A comprehensive analysis of all influencing variables was beyond the scope of this paper, but it proposes a new methodology to investigate those uncertainties that have not been discussed in the literature to date.

The following limitations of this study show how difficult it is to assess the uncertainty that arises from the measurement setup: the study is based on one case study that was associated with certain boundary conditions, e.g., a certain cloud base height that varied between 800 and 900 m. The yearly average cloud base height of low-level, single layer, liquid clouds at JOYCE-CF is about 1.2 km [17]. Increasing the cloud base height had the following effects: the uncertainty due to sensor displacement would decrease because of better beam overlap at larger altitudes. How the uncertainty changes due to different HPBW in this case depends on the ratio between the horizontal scale of cloud variability and the footprint of the instruments within the cloud. Additional parameters that can affect our analysis are the assumptions on DSD and effective radii, both influencing Z_e. Furthermore, we present uncertainty estimates in relative

units. However, knowing the absolute uncertainty is important when calculating physical quantities that are not linearly related to LWC.

The case scenario shown here is an idealized case because both instruments observe always the same scene, yet, with a spatial shift (time delay in observations). Moreover, steady state was assumed. Both aspects are very special cases, hence, cannot be generalized. It is likely that the uncertainties will be larger in a non-idealized case than the one presented here. One of the new findings of this study is that increasing the HPBW of the MWR increases the uncertainty of the retrieval by 3%–5%, as long as both sensors are located at the same position. If the instruments are displaced from each other, a wider MWR beam will be beneficial to sustain at least partial beam overlap, yet, the effect of displacement will contribute most to the retrieval error leading to uncertainties up to 30% at 100-m displacement.

To put the results of this study into the context of state-of-the-art instrumentation, we discuss our results in the following with respect to currently available technology while neglecting uncertainties of the LWC retrieval after [13]. The latter will be discussed at the end of this section. Combining an MWR, measuring between 20 and 31 GHz (K-band), with a co-located radar, measuring around 30 GHz, is a common approach to derive LWC profiles [8]. In the best case, both instruments are located within a few meters distance up to 10 m, which would lead to 10% relative uncertainty. In addition to that, a further uncertainty of about 40% due to the LWP retrieval must be considered, when assuming an uncertainty of 20 g m^{-2} [27] and an average LWP of 50 g m^{-2} (as given in the used case study). The latter was found to occur in various climate regimes [28]. The retrieval uncertainty of 20 g m^{-2} refers to a bias-free LWP retrieval that includes a thorough offset correction [29].

To our knowledge, the W-band radar used here to construct the reference cloud case is the only instrument combining radar and MWR measurements using the same antenna. Thus, the retrieval uncertainty is determined by the accuracy of the LWP retrieval and the radar noise (neglecting LWC retrieval uncertainties). For the LWP retrieval combining BT at 89 GHz and an *a priori* determined integrated water vapor (IWV), an uncertainty of 15 g m^{-2} was found by [17], when a thorough bias correction is applied. In this study, radar reflectivities were simulated only at 35 GHz for simplicity, so that attenuation effects could be neglected. However, at 94 GHz attenuation must be taken into account as further uncertainty source, which depends on LWC, IWV, and cloud thickness. A back-of-the-envelope calculation yielded that the relative error of LWC varies between 0% and 15% for LWP values between 25 and 250 g m^{-2}, a cloud thickness of 300 m and an IWV of 10 kg m^{-2}. Hence, a retrieval uncertainty between 30% and 45%, depending on attenuation (corrections), is expected when using a W-band radar–radiometer with matched beams. Because of the uncertainties associated with attenuation effects, we cannot make a general statement about which of the two measurement setups, i.e., W-band radar–radiometer or MWR at K-band frequencies plus a co-located radar, is the better choice to retrieve LWC in stratified of clouds. Yet, the results indicate that matched beams have the potential to decrease the retrieval uncertainty by 10% and more compared to a two-instrument setup, depending on the distance between radar and MWR.

Note that the uncertainties found here are only based on the instrument setup; however, do not include any biases in the retrieval assumptions themselves such as that the third moment of the DSD must be linearly related to the sixth moment of the DSD and that the droplet number concentration must be constant with height [30]. This becomes even more important for retrievals that require more information than radar reflectivity profiles and BTs. For instance, it was shown by [31] that it is key to characterize *a priori* information correctly to ensure reliable retrieval results of LWC when using probabilistic approaches. The need for accurate *a priori* estimates leads back to the investigations presented here: we need to quantify the uncertainties of our measurement setups to be able to collect reliable data sets that can serve as *a priori* estimates.

Finally, we show that cloud edge studies require closely matched beams in case of sharp cloud edges. Already at a displacement of 10 m, LWC profiles were associated with uncertainties larger than 75% or could not be derived at all due to missing LWP estimates. How much this uncertainty is at smoother cloud edges will be part of future work. Future studies should also investigate the influence of vertical resolution on the retrieval accuracy, especially, in less homogeneous cloud conditions.

Acknowledgment

The observational data used in this study are available at the Institute for Geophysics and Meteorology of the University of Cologne. Thanks to EMK for mental support.

References

[1] W. B. Rossow and R. A. Schiffer, "Advances in understanding clouds from ISCCP," *Bull. Am. Meteorol. Soc.*, vol. 80, no. 11, pp. 2261–2287, 1999.

[2] O. Boucher *et al.*, "7. clouds and aerosols," Climate Change 2013: Physical Sci. Basis. Contribution Working Group I Fifth Assessment Rep. Intergovernmental Panel Climate Change, pp. 571–657, 2013.

[3] R. A. J. Neggers, T. Heus, and A. P. Siebesma, "Overlap statistics of cumuliform boundary-layer cloud fields in large-eddy simulations," *J. Geophys. Res. Atmos.*, vol. 116, no. 21, pp. 1–10, 2011.

[4] A. S. Frisch, C. W. Fairall, and J. B. Snider, "Measurement of stratus cloud and drizzle parameters in ASTEX with a Ka-band doppler radar and a microwave radiometer," *J. Atmos. Sci.*, vol. 52, no. 16, pp. 2788–2799, 1995.

[5] U. Löhnert, S. Crewel, C. Simmer, and A. Macke, "Profiling cloud liquid water by combining active and passive microwave measurements with cloud model statistics," *J. Atmos. Ocean. Technol.*, vol. 18, no. 8, pp. 1354–1366, 2001.

[6] T. P. Ackerman and G. M. Stokes, "The atmospheric radiation measurement program," *Phys. Today*, vol. 56, no. 1, p. 38, 2003. [Online]. Available: https://doi.org/10.1063/1.1554135

[7] A. J. Illingworth *et al.*, "Cloudnet: Continuous evaluation of cloud profiles in seven operational models using ground-based observations," *Bull. Am. Meteorol. Soc.*, vol. 88, no. 6, pp. 883–898, 2007.

[8] U. Löhnert *et al.*, "JOYCE: Jülich observatory for cloud evolution," *Bull. Am. Meteorol. Soc.*, vol. 96, no. 7, pp. 1157–1174, 2015. [Online]. Available: http://journals.ametsoc.org/doi/abs/10.1175/BAMS-D-14-00105.1

[9] B. Stevens *et al.*, "The barbados cloud observatory—Anchoring investigations of clouds and circulation on the edge of the ITCZ," *Bull. Am. Meteorol. Soc.*, vol. 97, pp. 787–801, 2016. [Online]. Available: http://journals.ametsoc.org/doi/abs/10.1175/BAMS-D-14-00247.1

[10] C. Zhao *et al.*, "Toward understanding of differences in current cloud retrievals of ARM ground-based measurements," *J. Geophys. Res. Atmos.*, vol. 117, no. 10, 2012, doi: 10.1029/2011JD016792.

[11] G. Maschwitz, U. Löhnert, S. Crewell, T. Rose, and D. D. Turner, "Investigation of ground-based microwave radiometer calibration techniques at 530 hPa," *Atmos. Meas. Technol.*, vol. 6, no. 10, pp. 2641–2658, 2013.

[12] V. Meunier, U. Löhnert, P. Kollias, and S. Crewell, "Biases caused by the instrument bandwidth and beam width on simulated brightness temperature measurements from scanning microwave radiometers," *Atmos. Meas. Technol.*, vol. 6, no. 5, pp. 1171–1187, 2013.

[13] A. S. Frisch, G. Feingold, C. W. Fairall, T. Uttal, and J. B. Snider, "On cloud radar and microwave radiometer measurements of stratus cloud liquid water profiles," *J. Geophys. Res. Atmos.*, vol. 103, no. 18, pp. 23195–23197, 1998.

[14] S. Frisch, M. Shupe, I. Djalalova, G. Feingold, and M. Poellot, "The retrieval of stratus cloud droplet effective radius with cloud radars," *J. Atmos. Ocean. Technol.*, vol. 19, no. 6, pp. 835–842, 2002.

[15] U. Görsdorf *et al.*, "A 35-GHz polarimetric doppler radar for long-term observations of cloud parameters-description of system and data processing," *J. Atmos. Ocean. Technol.*, vol. 32, no. 4, pp. 675–690, 2015.

[16] J. Delanoë *et al.*, "BASTA: A 95-GHz FMCW doppler radar for cloud and fog studies," *J. Atmos. Ocean. Technol.*, vol. 33, no. 5, pp. 1023–1038, 2016. [Online]. Available: https://dx.doi.org/10.1175/JTECH-D-15-0104.1

[17] N. Küchler, S. Kneifel, U. Löhnert, P. Kollias, H. Czekala, and T. Rose, "A W-band radarradiometer system for accurate and continuous monitoring of clouds and precipitation," *J. Atmos. Ocean. Technol.*, vol. 34, no. 11, pp. 2375–2392, 2017. [Online]. Available: http://journals.ametsoc.org/doi/10.1175/JTECH-D-17-0019.1

[18] T. Rose, S. Crewell, U. Löhnert, and C. Simmer, "A network suitable microwave radiometer for operational monitoring of the cloudy atmosphere," *Atmos. Res.*, vol. 75, no. 3, pp. 183–200, 2005.

[19] R. Ware *et al.*, "A multichannel radiometric profiler of temperature, humidity, and cloud liquid," *Radio Sci.*, vol. 38, no. 4, pp. 44-1–44-13, 2003. [Online]. Available: http://doi.wiley.com/10.1029/2002RS002856

[20] A. Macke *et al.*, "The HD(CP)2 observational prototype experiment (HOPE) - An overview," *Atmos. Chem. Phys.*, vol. 17, no. 7, pp. 4887–4914, 2017.

[21] S. Kneifel, A. Lerber, J. Tiira, D. Moisseev, P. Kollias, and J. Leinonen, "Observed relations between snowfall microphysics and triple-frequency radar measurements," *J. Geophys. Res. Atmos.*, vol. 120, no. 12, pp. 6034–6055, 2015.

[22] D. L. Sisterson, R. A. Peppler, T. S. Cress, P. J. Lamb, and D. D. Turner, "The ARM southern great plains (SGP) site," *Meteor. Mon.*, vol. 57, pp. 6.1–6.14, 2016. [Online]. Available: http://journals.ametsoc.org/doi/10.1175/AMSMONOGRAPHS-D-16-0004.1

[23] G. L. Stephens, G. W. Paltridge, and C. M. R. Platt, "Radiation profiles in extended water clouds. III: Observations," *J. Atmos. Sci.*, vol. 35, no. 11, pp. 2133–2141, 1978. [Online]. Available: http://journals.ametsoc.org/doi/abs/10.1175/1520-0469%281978%29035%3C2133%3ARPIEWC%3E2.0.CO%3B2

[24] S. Crewell *et al.*, "Microwave radiometer for cloud carthography: A 22-channel ground-based microwave radiometer for atmospheric research," *Radio Sci.*, vol. 36, no. 4, pp. 621–638, 2001.

[25] M. Maahn, U. Löhnert, P. Kollias, R. C. Jackson, and G. M. McFarquhar, "Developing and evaluating ice cloud parameterizations for forward modeling of radar moments using in situ aircraft observations," *J. Atmos. Ocean. Technol.*, vol. 32, no. 5, pp. 880–903, 2015. [Online]. Available: http://journals.ametsoc.org/doi/abs/10.1175/JTECH-D-14-00112.1

[26] N. L. Miles, J. Verlinde, and E. E. Clothiaux, "Cloud droplet size distributions in low-level stratiform clouds," *J. Atmos. Sci.*, vol. 57, no. 2, pp. 295–311, 2000.

[27] U. Löhnert and S. Crewell, "Accuracy of cloud liquid water path from ground-based microwave radiometry 1. Dependency on cloud model statistics," *Radio Sci.*, vol. 38, no. 3, pp. 1–11, 2003.

[28] D. D. Turner, S. A. Clough, J. C. Liljegren, E. E. Clothiaux, K. E. Cady-Pereira, and K. L. Gaustad, "Retrieving liquid water path and precipitable water vapor from the atmospheric radiation measurement (ARM) microwave radiometers," *IEEE Trans. Geosci. Remote Sens.*, vol. 45, no. 11, pp. 3680–3690, Nov. 2007.

[29] K. Ebell, U. Löhnert, E. Päschke, E. Orlandi, J. H. Schween, and S. Crewell, "A 1-D variational retrieval of temperature, humidity, and liquid cloud properties: Performance under idealized and real conditions," *J. Geophys. Res. Atmos.*, vol. 122, no. 3, pp. 1746–1766, 2017. [Online]. Available: https://doi.org/10.1002/2016JD025945

[30] N. Küchler, S. Kneifel, U. Löhnert, and P. Kollias, "Revisiting liquid water content retrievals in warm stratified clouds: The modified frisch," *Geophys. Res. Lett.*, vol. 45, no. 17, pp. 9323–9330, 2018. [Online]. Available: https://doi.org/10.1029/2018GL079845

[31] K. Ebell, U. Löhnert, S. Crewell, and D. D. Turner, "On characterizing the error in a remotely sensed liquid water content profile," *Atmos. Res.*, vol. 98, no. 1, pp. 57–68, 2009. [Online]. Available: https://doi.org/10.1016/j.atmosres.2010.06.002

Nils Küchler was born in Karlsruhe, Germany. He received the B.S. degree in geophysics and meteorology, in 2012, the M.S. degree in physics of the atmosphere and the Ph.D. degree in meteorology from the University of Cologne, Cologne, Germany, in 2015 and 2019, respectively.

From 2015 to 2018, he was a Research Scientist with the University of Cologne. His work focused on ground-based remote sensing of low-level warm stratified clouds.

Ulrich Löhnert received the Ph.D. degree in meteorology from the University of Bonn, Bonn, Germany, in 2002. In 2012, he received the habilitation degree from the Faculty of Mathematics and Natural Sciences, University of Cologne, Cologne, Germany.

From 1998 to 2003, he was a Research Scientist with the University of Bonn, the University of Kiel, and the National Oceanic and Atmospheric Administration, Environmental Technology Laboratory. From 2004 to 2006, he was with the Ludwig-Maximilians-University of Munich, Munich, Germany, as an Assistant Professor. Since 2006, he has been a Senior Lecturer with the University of Cologne. In recent years, his research has focused on the development of statistical and physical methods for deriving profiles of the atmospheric thermodynamic state through sensor synergy, as well as on the retrieval of ice microphysical properties.